Novel and Conventional Techniques for Analyzing Fracture Fabrics

S.R. Ogilvie[1] , J.M. Orribo [1,2], P.W.J. Glover[1] and C. W. Taylor [1]

[1]Department of Geology and Petroleum Geology, University of Aberdeen, Aberdeen, Scotland
[2] Petroleum of Venezuela (PDVSA), Caracas, Venezuela

Abstract. The gross physical properties of rocks are controlled to a large extent by their deformational fabric, and particularly by faults, fractures and cataclastic deformation bands (DBs). These discontinuities within the rock often have a large impact upon the flow of fluids through the rock, acting as either conduits for or barriers to fluid flow. We have used a range of novel and conventional techniques to analyse sandstones containing DBs from the Inner Moray Firth Basin and Southern Permian Basin of the North Sea. Pressure Decay Profile Permeametry (PDPK) has been used to map the 2D permeability. Fluid flow has been monitored using positron emission tomography (PET) of core plugs. Conventional techniques such as porisimetry, permeametry, grain size analysis, SEM, cold cathodoluminesence, optical image analysis and mercury injection capillary pressure measurements have been used to give a robust characterisation of DB properties and to support the new measurements. It is demonstrated that using a variety of techniques to measure the same property considerable differences are observed, which are a function of the resolution of the techniques. There are also marked differences as a result of increasing the resolution.

Conclusions. From results of conventional and novel analysis measurements, considerable reductions in porosity and permeability occur within DBs compared to Host Rock (HR), which are the result of grain size reductions, clay mixing and cementation. This is accompanied by reductions in storage capacity and significant increases in irreducible water saturation and capillary pressures. These variations are dependant upon both HR composition and the scale of measurement. Despite the 2D nature of measurement, the high resolution PDPK and image analysis techniques enable observation of significant porosity and permeability anisotropy at the mm-scale compared to these properties measured at the cm-scale. However, PET scanning with low resolution has proven to be a successful technique to visualize the influence of DBs as potential barriers to fluid flow. Grain size reductions are modelled using a stochastic fragmentation model successfully reproducing the calculated distribution. The results of this study provide a detailed characterization of deformation bands with a variety of techniques which compliment each other at different resolutions. These results can be included in advanced reservoir simulation models.

1.1 Microstructural Analysis

1.1.1 SEM - BSEI

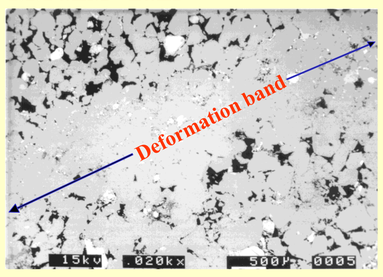

1.1.2 SEM - SE

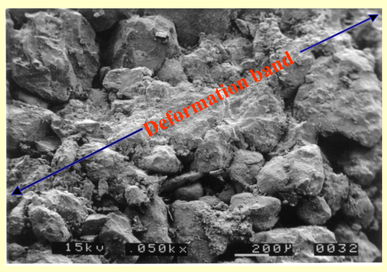

1.1.3 Thin section

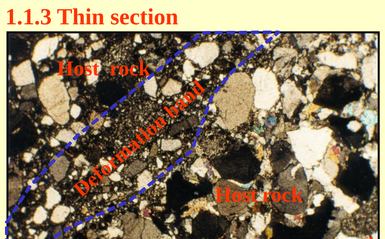

1.1.4 CL

1.2 Conventional Core Analysis

1.2.1 Petrophysical properties

Sample number	Sample Location	Swi (%)	Porosity (%)			Klinkenberg Permeability (mD)	
		MICP	Helium	MICP	Image analysis	Kn	PDPK
1	Deformation band	62.5	13.3	9.01	4 - 10	555	0.0034 - 397
2	Transitional	23.2	20.5	18.35	10 - 15	677	29.6 - 899
3	Host rock	11.3	25	19.95	15 - 21	1750	397 - 3080

1.2.2 Capillary pressure curves

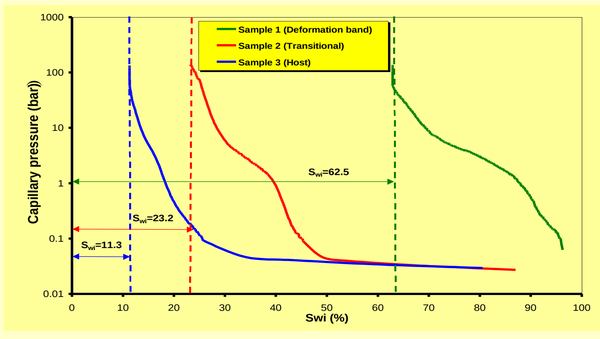

1.2.3 S_{wi} and storage capacity

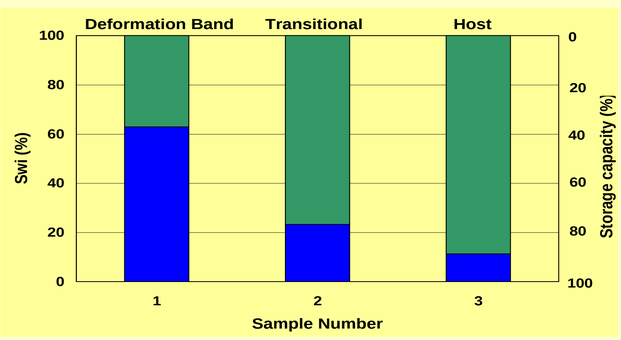

1.1 Microstructural Analysis of Deformation Bands (DB). 1.1.1. Scanning Electron Microscope (SEM) - Backscattered Electron Image (BSEI), showing dramatic reductions in porosity and grain size. 1.1.2. SEM- Secondary Electron (SE) image, highlighting the grain-size reductions at higher resolution. 1.1.3. Thin-section image of DB, in which the clay content contributes to the porosity reduction. 1.1.4. Cathodoluminesence (CL) image of a DB with fluorite cement, which also contributes to the porosity reduction. **1.2 Conventional Core Analysis of DB.** 1.2.1. Petrophysical properties of Host Rock (HR), DB and transitional samples; using Mercury Injection Capillary Pressure (MICP), Helium porosimetry, Image analysis porosimetry, Nitrogen permeametry (Kn) and Pressure Decay Profile Permeametry (PDPK). Variations in these properties for three samples can be seen in the table. 1.2.2. MICP-derived capillary pressure curves for these samples, showing significant variations. 1.2.3 Irreducible water saturation (S_{wi}) and storage capacity of the samples highlighting their considerable differences.

2.1 Pressure-Decay Profile Permeametry

2.1.1

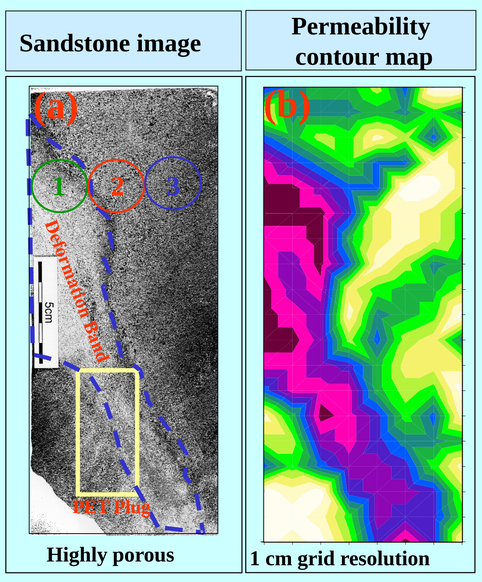

2.1.2

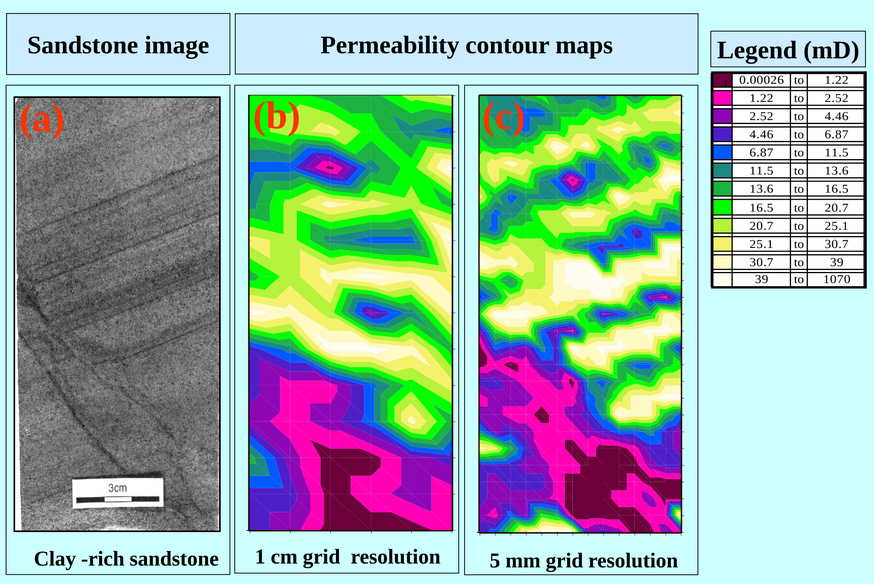

2.2 Grain Size Modelling

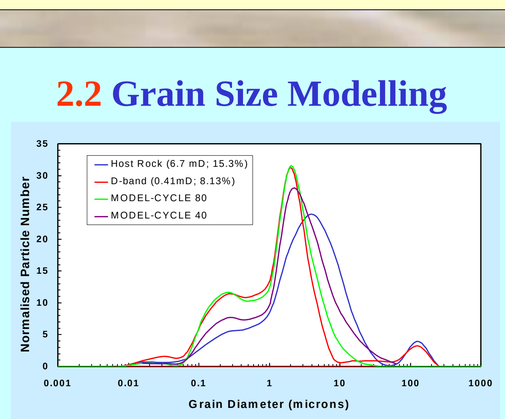

2.3 Image Analysis Porosity

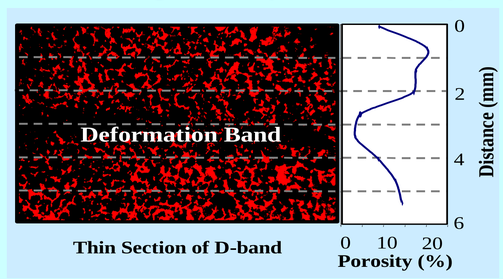

2.1 Pressure-Decay Profile Permeametry of DB zones. 2.1.1. (a) Porous sandstone containing a zone of DBs; (b) Permeability contours at 1cm grid resolution, showing up to 6 orders of magnitude reduction from HR to DB zones. 2.1.2. (a) Low-porosity sandstone containing a clay-rich DB zone; (b) Permeability contours at 1 cm grid resolution, also showing up to 6 orders of magnitude reduction; (c) At 5 mm grid resolution, showing a more detailed portrayal of the HR clay laminae and the DB zone. **2.2 Grain Size Modelling.** Based on "the theory of nearest neighbour", modelling of DB grain size distribution data was successfully achieved after 80 iterations. **2.3 Image Analysis Porosity.** The 2D porosity (in red) from HR into DB is calculated in 6 regions using image analysis software. This shows up to 75% reductions in porosity in the DB relative to the HR.

3.1 Positron Emission Tomography (PET)-Scanning

3.1.1

3.1.2

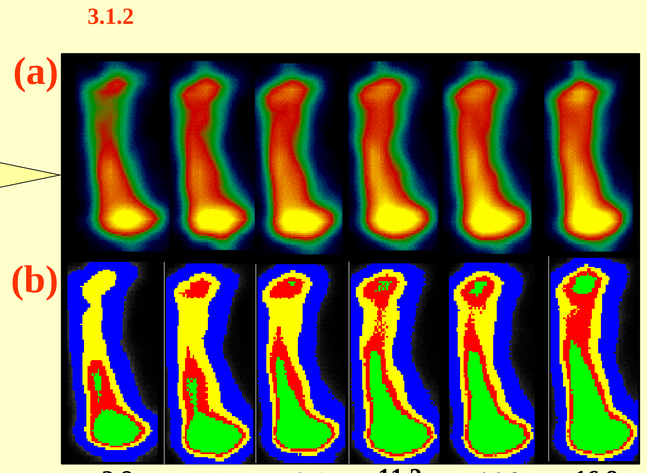

3.1.3

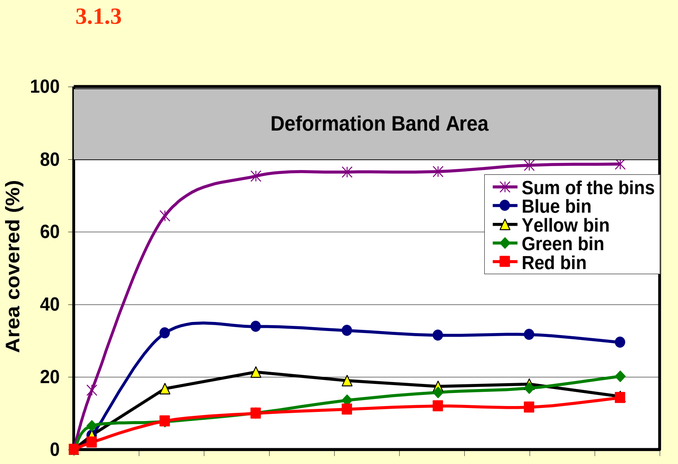

3.1 Positron Emission Tomography (PET)-Scanning. 3.1.1. Placement of the sandstone plug (Fig. 2.1.1a) with DBs into the PET scanner. 3.1.2. PET scanning images as a function of injected pore volume (P.V) and time, showing the concentration of the radioactive fluid through a cross-section of the plug cut obliquely to a DB zone (a) Images highlighting the influence of DB zone as a barrier to fluid flow (from top left to bottom right). (b) Distribution of radioactive concentration ranges (normalized bins), showing internal radioactive displacements with time. 3.1.3. Percentage of the area covered by the radioactive fluid and by each of the four normalized radioactive bins. This illustrates that the DB is compartmentalizing approximately 20% of the total area of the cross-section.

Contacts:
S.R. Ogilvie, e-mail: s.ogilvie@abdn.ac.uk.
J.M. Orribo, e-mail: t01jmo@abdn.ac.uk.
P.W.J. Glover, e-mail: p.glover@abdn.ac.uk.

Acknowledgments:
We would like to thank Conoco UK Ltd for sponsoring this work and Core Laboratories UK Ltd at Aberdeen for the use of their PDPK equipment. We are also grateful to Andrew Welch and Felice Chilcott (Biomedical Physics Dept., University of Aberdeen) for their assistance during the operation of the PET scanner.